

PARTIAL SUMS OF THE SERIES FOR THE DIRICHLET ETA FUNCTION, THEIR PECULIAR CONVERGENCE, THE SIMPLE ZEROS CONJECTURE, AND THE RH.

LUCA GHISLANZONI

luca.ghislanzoni@c-sigma.it

ABSTRACT. For any $s \in \mathbb{C}$ with $\Re(s) > 0$, denote by $\eta_{n-1}(s)$ the $(n-1)^{th}$ partial sum of the Dirichlet series for the eta function $\eta(s) = 1 - 2^{-s} + 3^{-s} - \dots$, and by $R_n(s)$ the corresponding remainder. Denoting by $u_n(s)$ the segment starting at $\eta_{n-1}(s)$ and ending at $\eta_n(s)$, we first show how, for sufficiently large n values, the circle of diameter $u_{n+2}(s)$ lies strictly inside the circle of diameter $u_n(s)$, to then derive the asymptotic relationship $R_n(s) \sim (-1)^{n-1}/n^s$, as $n \rightarrow \infty$. Denoting by $D = \{s \in \mathbb{C} : 0 < \Re(s) < \frac{1}{2}\}$ the open left half of the critical strip, define for all $s \in D$ the ratio $\chi_n^\pm(s) = \eta_n(1-s)/\eta_n(s)$. We then prove that the limit $L(s) = \lim_{N(s) < n \rightarrow \infty} \chi_n^\pm(s)$ exists at every point s of the domain D . The function $L(s)$ is continuous on D if and only if the Riemann Hypothesis is true. Finally, we remark how the asymptotic behavior of $R_n(s)$ can also provide insights substantiating the so called Simple Zeros Conjecture.

1. INTRODUCTION

On the 11th of August 1859, Bernhard Riemann was appointed member of the Berlin Academy. Respectful of such great honor, Riemann submitted to the Academy his seminal work on the distribution of prime numbers less than a given quantity (Über die Anzahl der Primzahlen unter einer gegebenen Grösse, [1]). In that paper Riemann formulated a daring hypothesis [2]:

All non-trivial zeros of the zeta function lie on the critical line

Denoted by $s = \sigma + it$ a complex number, said Riemann Zeta function, $\zeta(s)$, is the function defined as the analytic continuation to all the complex values $s \neq 1$ of the infinite series:

$$(1) \quad \zeta(s) = \sum_{n=1}^{\infty} \frac{1}{n^s} = 1 + \frac{1}{2^s} + \frac{1}{3^s} + \frac{1}{4^s} + \dots,$$

which converges only in the half-plane $\Re(s) > 1$. $\zeta(s)$ has zeros at $s = -2, -4, -6, \dots$, which are called *trivial zeros* because their existence is easy to prove. The Riemann zeta function features also other zeros, called *non-trivial zeros*, known to lie in the open strip $s \in \mathbb{C} : 0 < \Re(s) < 1$, which is called the *critical strip*. The *critical line* is then defined as the line $s \in \mathbb{C} : \Re(s) = \frac{1}{2}$. The Riemann Hypothesis asserts that all *non-trivial zeros* lie on the critical line.

Since Riemann's milestone paper the properties of $\zeta(s)$ have been studied in much depth. Besides Riemann's own results on the distribution of prime numbers, the Riemann Hypothesis has important implications also for a number of problems in physics [3]. From the great wealth of existing literature only few key definitions and results are recalled in this introduction. This work will then concentrate its attention on the behavior of the zeros of $\zeta(s)$ in the interior of the critical strip.

A key role in the analytical continuation to $\Re(s) > 0$ of the series (1) is played by the Dirichlet Eta function [4]:

$$(2) \quad \eta(s) = \sum_{n=1}^{\infty} \frac{(-1)^{n-1}}{n^s} = 1 - \frac{1}{2^s} + \frac{1}{3^s} - \frac{1}{4^s} + \dots$$

The above series represents the simplest alternating signs case among Ordinary Dirichlet Series, and it is converging for all s with $\Re(s) > 0$. Its sum, $\eta(s)$, is an analytic function in the corresponding half-plane.

Analytic continuation to $\Re(s) > 0$ of the infinite series (1) can then be obtained by observing that:

$$(3) \quad \zeta(s) = \frac{\eta(s)}{1 - \frac{2}{2^s}},$$

which is valid for $s \neq 1 + n \cdot \frac{2\pi}{\ln 2} i$ ($n \in \mathbb{Z}$), values at which the denominator vanishes.

The right hand side of (3) is analytic in the region of interest for this work: the interior of the critical strip. Inside such region, the zeros of the Riemann ζ coincide with the zeros of the η function. As the infinite sum (2) converges readily, it makes it easy to graphically represent the path described by the partial sums.

Let us denote the partial sums as $\eta_{k-1}(s)$ and the corresponding remainder as $R_k(s)$ so defined:

$$(4) \quad \sum_{n=1}^{\infty} \frac{(-1)^{n-1}}{n^s} = \sum_{n=1}^{k-1} \frac{(-1)^{n-1}}{n^s} + \sum_{n=k}^{\infty} \frac{(-1)^{n-1}}{n^s} = \eta_{k-1}(s) + R_k(s),$$

The terms of the infinite sum (2) are complex numbers, which can be represented by vectors of the form $u_n(s) = (-1)^{n-1} \frac{1}{n^\sigma} e^{-it \ln n}$. The line segments making up the paths graphed in Fig. 1 represent said vectors added up "tip to tail". As it will be better detailed in the proof of **Theorem 1**, while approaching the point of convergence, $\eta(s)$, the path described by the partial sums eventually ends up following a very simply structured *star-shaped* path (depicted in the square inset at the top left of Fig. 1), characterized by angles between consecutive segments being $< \frac{\pi}{2}$, getting smaller and smaller as n grows larger and larger.

A remarkable functional equation satisfied by $\zeta(s)$ was originally proposed by Euler in 1749, and later proved by Riemann in his 1859 paper [1] [5]

$$(5) \quad \zeta(1-s) = 2(2\pi)^{-s} \cos\left(\frac{\pi s}{2}\right) \Gamma(s) \zeta(s) \quad OR \quad \zeta(1-s) = \chi(s) \zeta(s).$$

When studying the behavior of $\zeta(s)$ inside the critical strip, a useful implication of (5) is that to $\zeta(s) = 0$ it must correspond $\zeta(1-s) = 0$. Therefore, if $s = \frac{1}{2} - \alpha + it$ ($0 \leq \alpha < \frac{1}{2}$) is a zero of $\zeta(s)$, then so it must be for both $1-s = \frac{1}{2} + \alpha - it$ and its complex conjugate $1-\bar{s} = \frac{1}{2} + \alpha + it$. Thus, non-trivial zeros always occur in groups of two pairs, one pair being the complex conjugate of the other, symmetrically located about the critical line. As this work is concerned with the study of the behavior of the zeros of $\zeta(s)$ in the interior of the critical strip, and inside such region a useful implication of (3) is that said zeros coincide with the zeros of $\eta(s)$, one could as well concentrate on the study of the behavior of pairs of critical line symmetrical zeros of the function $\eta(s)$, which also satisfies a functional equation, readily obtainable from (3) when restricting to the the open critical strip

$$(6) \quad \eta(1-s) = \frac{1-2^s}{1-2^{1-s}} 2(2\pi)^{-s} \cos\left(\frac{\pi s}{2}\right) \Gamma(s) \eta(s) \quad OR \quad \eta(1-s) = \chi^\pm(s) \eta(s).$$

whereby the \pm label is added because this is the functional equation for the alternating sign ζ function.

The readily converging sum (2) allows to easily visualize, by drawing the corresponding graphs, the paths described by the partial sums of critical line symmetrical arguments.

The pattern of convergence of the partial sums, $\eta_N(s)$, of the alternating Dirichlet series displays a beautiful and features rich geometrical structure, of which Fig.1 provides only an example (restricted to the first 1000 terms of the sum for $\eta\left(\frac{1}{2} \pm 0.15 + i2103.19\right)$). The red path is obtained by drawing the line segments, $u_N(s) = (-1)^{N-1}/N^s$ joining partial sum $\eta_{N-1}(s)$ with $\eta_N(s)$, while the green one is obtained by drawing the corresponding $u_N(1-\bar{s})$. The green path represents a sort of image of the red one, in the sense that each green $u_N(1-\bar{s})$ segment is by definition parallel to the corresponding red $u_N(s)$ segment, while being scaled down by $N^{2\sigma-1}$.

Imagine now to walk along one such path in the direction of increasing N . Upon arriving at the end of segment $u_N(s)$, in order to step on segment $u_{N+1}(s)$ we will then need to turn left or right, according to the value of the difference between their respective arguments, noting that $\theta_n(t) = -t \log n$ when n is odd, whereas $\theta_n(t) = \pi - t \log n$ when n is even. Thus, the included angle between $u_N(s)$ and $u_{N+1}(s)$ is $\delta_{N+1}(t) = t \log \frac{N+1}{N}$. Suppose we have already walked our way through that kind of "whirl" labeled as D, and we are thus turning to our right when stepping on the next segment, as soon as we arrive at the end

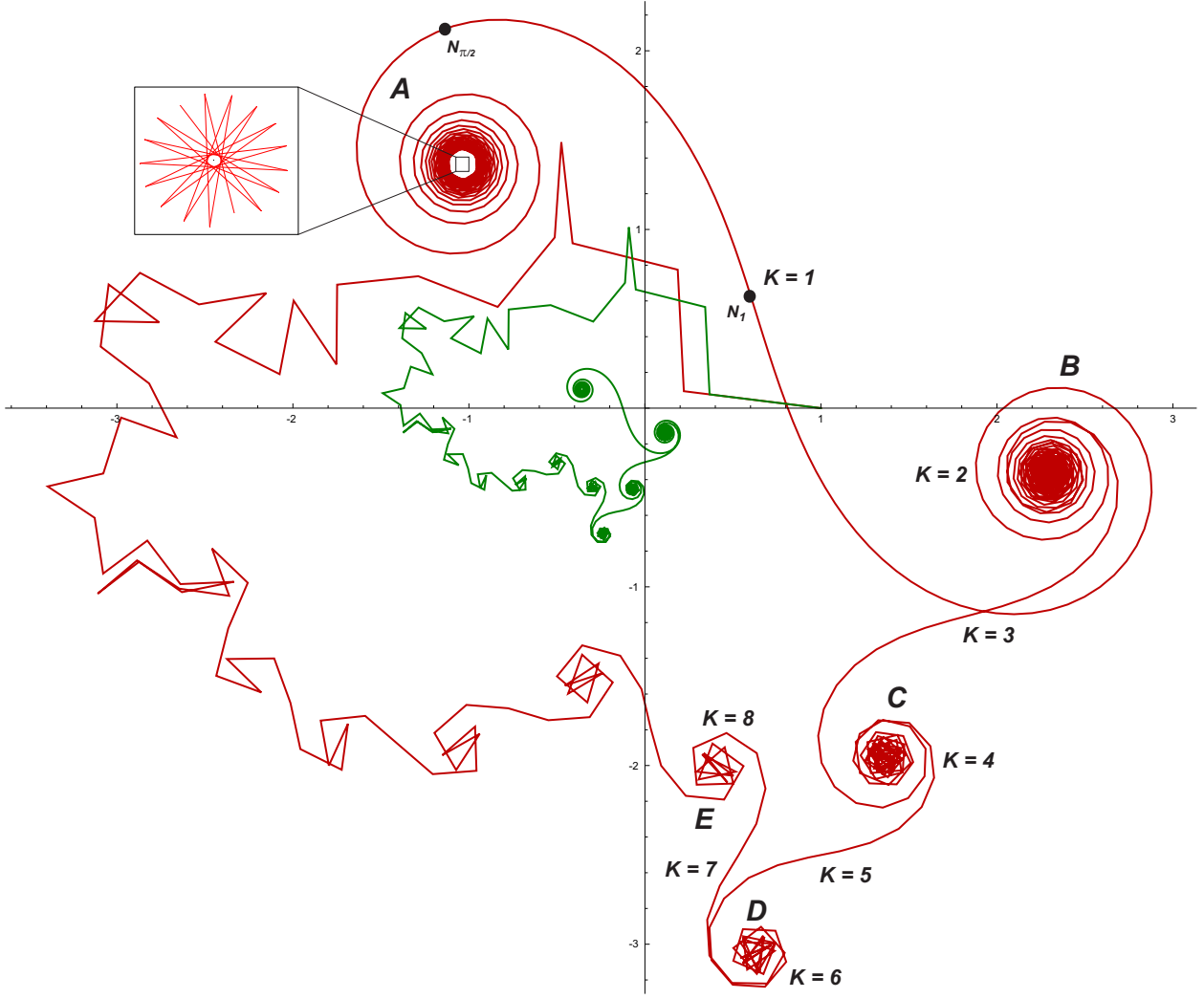


FIGURE 1. Paths described by the partial sums of the series for $\eta(s)$ and $\eta(1-\bar{s})$, $s = \frac{1}{2} - \alpha + it$.

of a segment for which $\delta_{N+1}(t)$ switches from the range of values $K\pi > \delta_{N+1}(t) > (K-1)\pi$, $K = 6$, to the range of values $5\pi > \delta_{N+1}(t) > 4\pi$ (i.e. $K = 5$), we will need to turn to the left. We would then return to take turns to the right somewhere in the middle of whirl C, when $\delta_{N+1}(t)$ crosses from range $K = 5$ into range $4\pi > \delta_{N+1}(t) > 3\pi$ (i.e. $K = 4$), and so on and so forth, until finally reaching the $K = 1$ range $\pi > \delta_{N+1}(t) > 0$, then forever taking turns to the left, while getting closer and closer to $\eta(s)$ (located somewhere in the middle of whirl A, which we can hence name *End Whirl*). The square inset enlarges a detail (for just 16 segments) as it would appear by zooming deep inside the *End Whirl*, revealing how it eventually settles into a very simply structured star-shaped pattern. K-range crossing from K into $K - 1$ occurs at the end of the u_{N_K} segment, where

$$(7) \quad N_K = \left\lceil \frac{1}{e^{\frac{K\pi}{t}} - 1} \right\rceil$$

Incidentally, the study of the size of said K-ranges may suggest a sufficient condition for the Lindelöf Hypothesis. The number of K-ranges is $K_{MAX} = t \log 2 / \pi$ (inverting 7 when $N_K = 1$). Were it possible to show that along the critical line the size of each K-range is bounded by $\frac{C}{k}$, $C > 0$ no matter how large, then:

$$(8) \quad |\eta(s)| < C \sum_{k=1}^{K_{MAX}} \frac{1}{k} = C(\log K_{MAX} + \gamma + \dots) = C \log t + C\gamma + C \log \frac{\log 2}{\pi} + \dots \rightarrow O(t^\epsilon)$$

Note that such $O(t^\varepsilon)$ behavior (Lindelöf Hypothesis for the Riemann Zeta function, but which directly transfers to the η function thanks to the fact that $\sqrt{3-2\sqrt{2}} \leq |1-2^{0.5-it}| \leq \sqrt{3+2\sqrt{2}}$) would still be preserved even if the constant C were instead a function of t growing no faster than $C(t) = c(\log t)^b$, $b > 0$ and $c > 0$ no matter how large.

2. THE GEOMETRIC APPROACH

By studying the geometrical pattern traced by the $\eta_n(s)$, it is possible to identify stricter bounds for the asymptotic size of the remainder $R_n(s)$. Said asymptotic size is already known to be of the order of its first term (for example through the application of Euler MacLaurin summation formula). Here we will instead follow a geometric approach resulting in a strict asymptotic relationship, while also producing some other interesting insights.

Theorem 1. *For $s = \sigma + it$ in the interior of the critical strip, denote by $\eta_{n-1}(s)$ the $(n-1)^{th}$ partial sum of the series for the η function, by $R_n(s)$ the corresponding remainder, and by $u_n(s)$ the line segment starting at $\eta_{n-1}(s)$ to end at $\eta_n(s)$. For sufficiently large n , it follows that*

$$\text{the circle of diameter } u_{n+2}(s) \text{ lies strictly inside that of diameter } u_n(s) ,$$

hence

$$(9) \quad |R_n(s)| < \frac{1}{n^\sigma}$$

moreover, a strict asymptotic relationship holds

$$(10) \quad \text{as } n \rightarrow \infty \quad R_n(s) = \frac{(-1)^{n-1}}{2n^s} + \varepsilon_n(s) , \quad \frac{\varepsilon_n(s)}{n^{-\sigma}} \rightarrow 0$$

actually, one even has $\varepsilon_n(s) \in o\left(\frac{1}{n^2}\right)$.

PROOF.

The procedure followed for this proof is based on a geometric analysis of the pattern of convergence displayed by the path traced by the partial sums $\eta_n(s)$. Said path is composed of line segments, and for simplicity we will use the term u_n to refer to the line segment starting at $\eta_{n-1}(s)$ and ending at $\eta_n(s)$, while implicitly assuming its dependence on s . Furthermore, because pair of paths corresponding to $s = \sigma + it$ and $\bar{s} = \sigma - it$ are mirror symmetrical with respect to the real axis, it will be sufficient to prove the following results for the case $t > 0$.

While approaching their respective point of convergence, $\eta(s)$, paths corresponding to different values of $\sigma > 0$ appear all to end up describing simply structured star-shaped patterns (recall the inset in Fig. 1), characterized by angles between consecutive segments being $< \frac{\pi}{2}$. This is actually the result of having to add π , to the argument $-t \ln(n)$, every other segment (because of the alternating sign). In fact, when n becomes sufficiently large, $t \ln(n+1)$ will be just a bit larger than $t \ln(n)$, and because one of the two segments will need to be turned around by π (the segment corresponding to even n), the angle between said consecutive segments will eventually become an acute angle $\delta_{n+1} = t \ln(n+1) - t \ln(n) < \frac{\pi}{2}$ (Fig. 3a helps in visualizing this), shrinking down more and more as n grows larger and larger. Being interested solely in the absolute value of said acute angle, it can be easily verified that its value is $|-t \ln \frac{n+1}{n}| = |t \ln \frac{n}{n+1}|$, which is the same as $t \ln \frac{n+1}{n}$ when $t \geq 0$, and hence $\rightarrow 0$ as $n \rightarrow \infty$. Ultimately, the observed star-shaped pattern is hence a direct result of the alternating signs in (2).

Fig. 2 illustrates an example, limited to just 3 consecutive segments, of how said pattern appears once the path described by the partial sums has already settled into the star-shaped pattern at the center of the *End Whirl* (Fig. 1). We will at first demonstrate that said star-shaped pattern ought to be bounded in size. To this end we construct a circle whose diameter is u_n , and whose center, C_n , is its the midpoint. Then, if the disk defined by the circle constructed in a similar way on u_{n+2} were eventually (i.e.: as $n \rightarrow \infty$) contained within the disk defined by the circle constructed on u_n , we would have proved that the distance between point $\eta_n(s)$ and the point of convergence, $\eta(s)$, cannot be greater than the length of u_n . Fig. 2a illustrates the geometric construction on which this proof will be based. As this proof is concerned solely

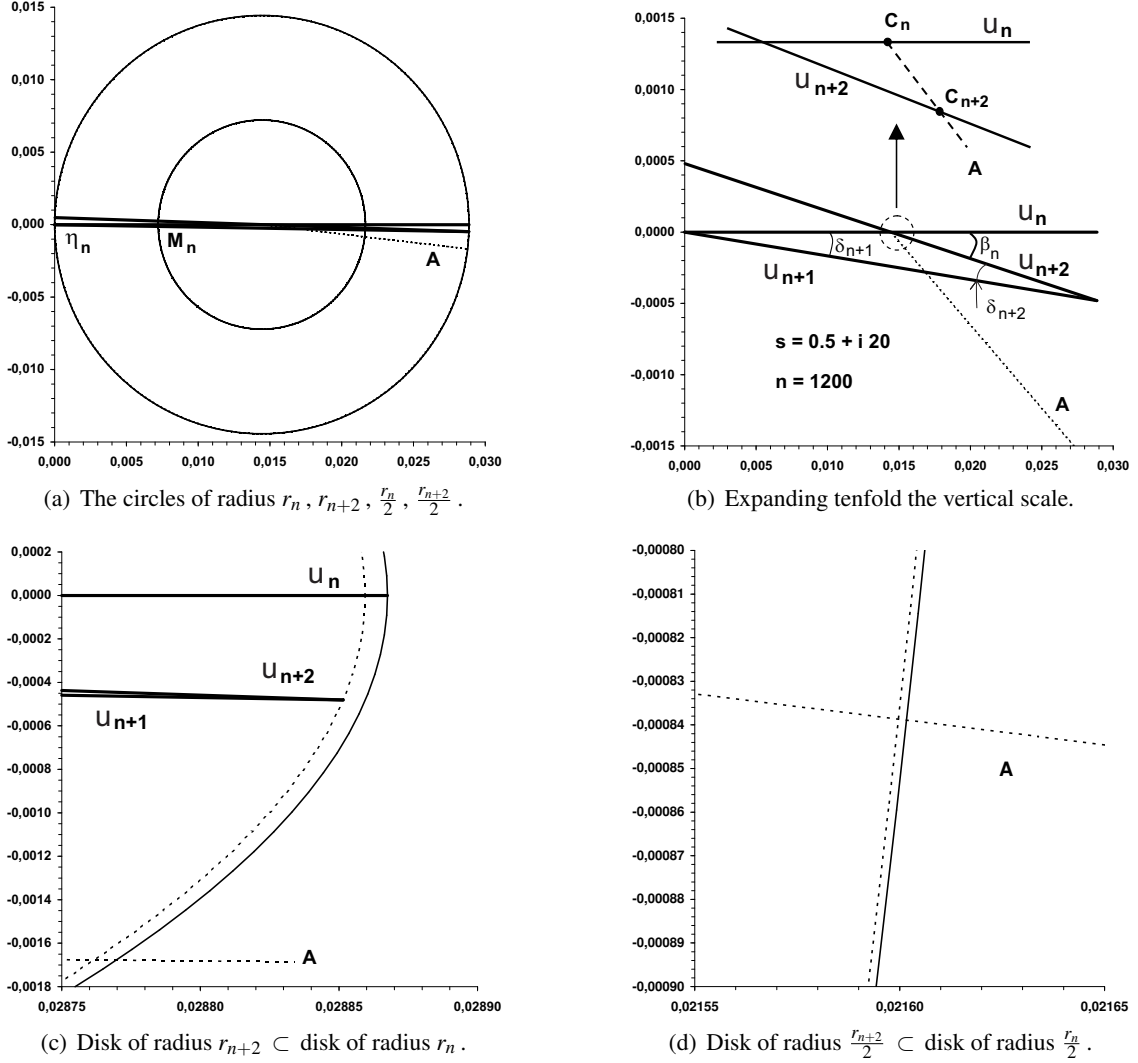


FIGURE 2. proving that $|R_n(\sigma + it)| \sim \frac{1}{2n^\sigma}$ as $n \rightarrow \infty$.

with the geometric relationships of u_n , u_{n+1} , and u_{n+2} , relatively to each other, our frame of reference can be chosen in any convenient way which preserves said relative properties. The origin of the frame of reference chosen for Fig.2 coincides with the point $\eta_n(s)$, while the real axis is chosen as to overlap u_n . In Fig. 2b the scale of the imaginary axis has been purposely stretched by a factor of 10, only to make it easier to visualize the pattern described by the partial sums. Referring to the triangle defined by the intersections of u_n , u_{n+1} , and u_{n+2} , let us denote by $\delta_{n+1} = t \ln \frac{n+1}{n}$ the angle between u_{n+1} and u_n , by $\delta_{n+2} = t \ln \frac{n+2}{n+1}$ the angle between u_{n+2} and u_{n+1} , and by β_n the supplement of the third angle of said triangle (i.e. the angle between u_n and u_{n+2}). By construction, angle β_n corresponds to $\beta_n = \delta_{n+1} + \delta_{n+2} = t \ln \frac{n+2}{n}$.

Fig. 2b shall then be read as follows:

u_n starts off at $\frac{1}{n^\sigma} + i0$, ending at $0 + i0$;

u_{n+1} starts off at $0 + i0$, ending at $\frac{1}{(n+1)^\sigma} (\cos \delta_{n+1} - i \sin \delta_{n+1})$;

u_{n+2} starts from the end of *segment* $n+1$, ending at $\frac{\cos \delta_{n+1}}{(n+1)^\sigma} - \frac{\cos \beta_n}{(n+2)^\sigma} + i \left(-\frac{\sin \delta_{n+1}}{(n+1)^\sigma} + \frac{\sin \beta_n}{(n+2)^\sigma} \right)$.

Line **A** is drawn through C_n and C_{n+2} , the midpoints of u_n and u_{n+2} (see the enlarged detail in Fig. 2b). C_n is also the center of the circle (solid line) having u_{n+2} as its diameter, and hence the radius of said circle is $r_n = \frac{1}{2n^\sigma}$. C_{n+2} is also the center of the circle (dotted line) having u_{n+2} as its diameter, and hence the radius of said circle is $r_{n+2} = \frac{1}{2(n+2)^\sigma}$. The purpose of line **A** is to make it easier to identify the points of closest approach of the two circles. In Fig. 2c said circles appear stretched. This is the result of having chosen different scale factors for the two axes, so that line **A** may also appear in the graph together with all other segments. It is clear that for the example of Fig.2 ($s = \frac{1}{2} + i20$, $n = 1200$) the disk of radius r_{1202} is contained within the disk of radius r_{1200} (closest approach is their distance along line **A**). Several other examples were verified by numerical simulations, always resulting in *disk* $n+2$ being eventually contained strictly inside *disk* n , and therefore suggesting that this kind of asymptotic behavior might indeed be representative of the most general case. To demonstrate that this is actually the case, any effective proof will need to rely solely on assumptions eventually satisfied, as $n \rightarrow \infty$, by the partial sums $\eta_n(\sigma + it)$. As a matter of fact, for values n such that $t \ln \frac{n+1}{n} < \frac{\pi}{2}$, any three consecutive segments will define a triangle of the same kind as the one depicted in Fig. 2b, and this irrespective of the particular value $\sigma > 0$ (more precisely, the triangle in Fig. 2b actually refers to δ_{n+1} and δ_{n+2} both $< \frac{\pi}{4}$, but it is easy to verify that (11), identifying the locations of C_n and C_{n+2} , are valid even when said angles are both just a tiny little bit less than $\frac{\pi}{2}$). We shall also remark that the validity of the following proof cannot possibly be affected by our choice to start from a line segment of even index, rather than from one of odd index.

The following proof will refer solely to values $n \geq N$, where $N = N(t)$ is the smallest integer that is not less than $1/(e^{\frac{\pi}{2t}} - 1)$. Let us first evaluate the distance $\Delta_c = \Delta_c(n) = |C_{n+2} - C_n|$

$$\begin{aligned}
C_n &= \frac{1}{2n^\sigma} + i0 & C_{n+2} &= \frac{\cos \delta_{n+1}}{(n+1)^\sigma} - \frac{\cos \beta_n}{2(n+2)^\sigma} + i \left(-\frac{\sin \delta_{n+1}}{(n+1)^\sigma} + \frac{\sin \beta_n}{2(n+2)^\sigma} \right) \\
\Delta_c^2 &= |C_{n+2} - C_n|^2 = \\
&= \frac{\cos^2 \delta_{n+1}}{(n+1)^{2\sigma}} + \frac{\cos^2 \beta_n}{4(n+2)^{2\sigma}} - \frac{\cos \delta_{n+1} \cos \beta_n}{(n+1)^\sigma (n+2)^\sigma} + \frac{1}{4n^{2\sigma}} + \frac{\cos \beta_n}{2n^\sigma (n+2)^\sigma} - \frac{\cos \delta_{n+1}}{n^\sigma (n+1)^\sigma} \\
&+ \frac{\sin^2 \delta_{n+1}}{(n+1)^{2\sigma}} + \frac{\sin^2 \beta_n}{4(n+2)^{2\sigma}} - \frac{\sin \delta_{n+1} \sin \beta_n}{(n+1)^\sigma (n+2)^\sigma} \\
(11) \quad &= \frac{1}{(n+1)^{2\sigma}} + \frac{1}{4(n+2)^{2\sigma}} - \frac{\cos(\beta_n - \delta_{n+1})}{(n+1)^\sigma (n+2)^\sigma} + \frac{1}{4n^{2\sigma}} + \frac{\cos \beta_n}{2n^\sigma (n+2)^\sigma} - \frac{\cos \delta_{n+1}}{n^\sigma (n+1)^\sigma} .
\end{aligned}$$

For the difference between the two radiuses, $\Delta_r = \Delta_r(n) = |r_n - r_{n+2}|$, we have

$$(12) \quad \Delta_r^2 = \frac{1}{4n^{2\sigma}} + \frac{1}{4(n+2)^{2\sigma}} - \frac{1}{2n^\sigma (n+2)^\sigma} .$$

Subtracting (11) from (12) and simplifying, $\Delta_r^2 - \Delta_c^2$ becomes

$$(13) \quad \frac{(1 + \frac{1}{n})^\sigma \left[(n+2)^\sigma \cos(\delta_{n+1}) - (n+1)^\sigma \frac{1 + \cos(\beta_n)}{2} \right] - \left[(n+2)^\sigma - (n+1)^\sigma \cos(\beta_n - \delta_{n+1}) \right]}{(n+1)^{2\sigma} (n+2)^\sigma} .$$

Considering that for any given t the cosine factors $\rightarrow 1 + O(1/n^2)$ as $n \rightarrow \infty$, both the square brackets at the numerator expand to $[(n+2)^\sigma - (n+1)^\sigma + O(n^{1-2/\sigma})]$, valid for any $0 < \sigma < 1$. Thus, the numerator is eventually a strictly positive quantity. However, at smaller n values the oscillatory nature of those cosine factors has a much greater impact, and it is not difficult to verify the existence of values of n resulting in (13) < 0 . Thus, because (13) $\rightarrow 0$ from eventually positive values, it means that there must exist a value of $h = h(\sigma, t)$ at which (13) definitely crosses over from negative to positive values. Fig. 3b plots (13) for the example $t = 300$, $\sigma = 0.65$, while for the general case it can be verified that said last crossing from negative to positive values occurs around $\frac{t^2}{2\sigma}$ (though tedious, it can be verified by expanding at $x = \frac{t^2}{2\sigma}$ to

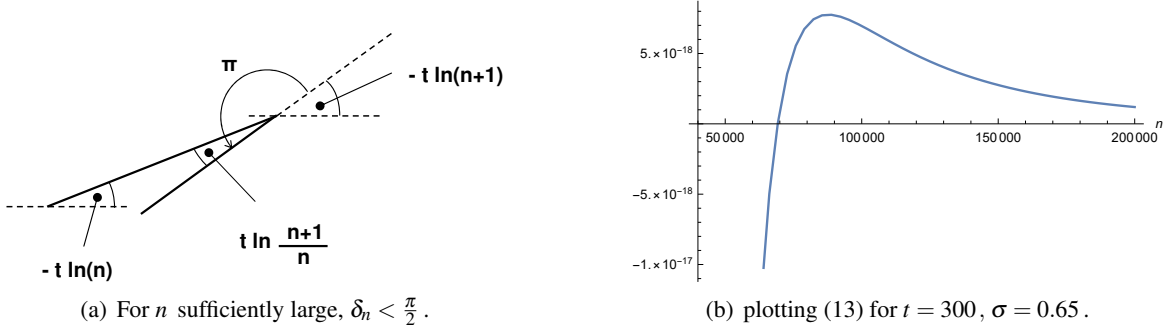


FIGURE 3

then observe the change of sign when increasing from $n = \lfloor x \rfloor - 1$ to $\lceil x \rceil + 1$, although such result will not be used here. For all values $n > h$ it is therefore $\Delta_r^2 - \Delta_c^2 > 0$, implying that Δ_r is eventually $\Delta_r > \Delta_c$, in turn implying that the circle built on *segment* $n + 2$ is strictly contained within the circle built on *segment* $n + 4$, the one built on *segment* $n + 4$ is strictly contained within that built on *segment* $n + 2$, and so on, as $n \rightarrow \infty$, while shrinking down to the point of convergence, $\eta(s)$, and thus proving (9).

By tediously expanding (11) for $n \rightarrow \infty$ it turns out that terms of the order $n^{-2\sigma}$ all cancel each other out, so that the next remaining terms are those of the order $n^{-4-2\sigma}$. Hence,

$$(14) \quad |C_{n+2} - C_n| = O\left(\frac{1}{n^{2+\sigma}}\right)$$

whereas, by definition, the diameters of the nested circles vanish at the $n^{-\sigma}$ rate. Thus, the distance (14) between the centers of two consecutive nested circles vanishes at a much faster rate than their diameters, in turn implying that the nested circles ought to be asymptotically concentric, finally proving (10). \square

In fact, by observing that $R_n(s)$ vanishes closer and closer to both C_n and C_{n+2} , implying that the error term $R_n(s) - n^{-s}/2$ cannot shrink slower than (14), by further remarking that $\sigma > 0$ we could as well conclude that $|R_n(s) - n^{-s}/2| \in o(n^{-2})$.

To aid in visualizing the result of **Theorem 1**, Fig. 4a illustrates the star shaped pattern drawn by connecting up consecutive values of $\eta_k(s_0)$ (i.e. the vertexes), for $s_0 = 1/2 + i 37.5861781588256$, the sixth non-trivial zero (at zeros, it is of course $\eta_{k-1}(s_0) = -R_k(s_0)$). It depicts solely partial sums featuring $k > \frac{t_0^2}{2\sigma_0}$, so that the circle of diameter $u_{k+2}(s_0)$ is strictly contained within the circle of diameters $u_k(s_0)$. It is apparent how $\eta(s_0) = 0$ is indeed located somewhere very near the centers of said nested circles. The pattern of convergence towards the "center" (using "center" to roughly indicate the point of convergence) of the star-shaped pattern can then be best appreciated when plotting only even-indexed partial sums (the grey dots in Fig. 4b), rather than each one of them (which will jump back and forth between nearly diametrically opposed positions, because of the alternating sign, as clearly illustrated by Fig. 4a). Similarly, this also holds when plotting only the odd-indexed ones.

Thus, without loss of generality, we will henceforth restrict our discussion to even values of N .

The smaller black dots in Fig. 4b represent instead the values computed using (10). By zooming in on Fig. 4b (the figures in this PDF allow zooming to a very fine level of detail), it becomes visually apparent that, as one moves toward the inner turns of the spiraling pattern (i.e., as k increases), the black dots overlap the gray ones with increasing accuracy. This provides numerical evidence supporting the result of **Theorem 1**. For convenience, in the following we will use the term *Deep Spiral N* to denote the pattern of convergence of the $R_{2k}(s)$, starting from index $2k = N$, where N is any sufficiently large value located deep inside the *End Whirl* and satisfying the condition "the circle of diameter $u_{N+2}(s)$ lies strictly inside that of diameter $u_N(s)$ ". Upon closer inspection, Fig. 4b reveals that the spacing between dots decreases as k increases, both in the radial direction and along the spiral itself. In polar coordinates, this corresponds to an increase in the

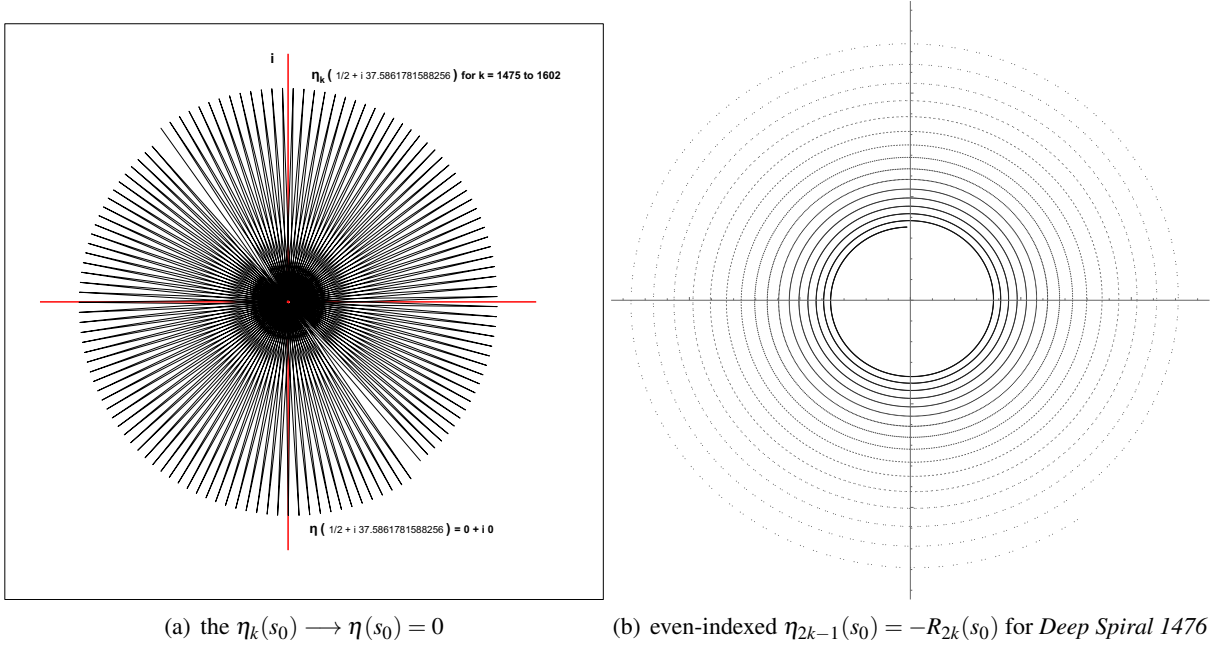


FIGURE 4. $\eta_k(s)$ examples at a known zero. At the right, when joining only even indexed $\eta_k(s)$.

density of dots along both the radial and angular coordinates. It is not difficult to show that this is a general result, independent of the particular choice of s_0 used in Fig. 4b. Let us consider the first full turn of *Deep Spiral N*, for sufficiently large N , the asymptotic expression (10) suggests that one 2π revolution along the spiral would very nearly correspond to a 2π rotation of $-1/(2k)^s$. Thus, starting at N , said 2π angular span is covered by index:

$$(15) \quad k = N + 2j, \quad 0 \leq j \leq m, \quad m = \lfloor N \left(e^{\frac{2\pi}{t}} - 1 \right) / 2 \rfloor \xrightarrow{t \rightarrow \infty} N \frac{\pi}{t}, \quad N > \frac{t^2}{2\sigma}$$

thus, m corresponds to the number of dots present in the first full 2π turn of *Deep Spiral N* (more exactly, the angular span nearest to 2π and $\leq 2\pi$). Notice how, at large t values, the length of the first turn of *Deep Spiral N* contracts at nearly the same rate as the circumference of the circle of diameter $1/N^\sigma$. We can hence estimate that the density of dots along the spiraling pattern grows at nearly the same rate as $N^{1+\sigma}/t$ (while it is $N > \frac{t^2}{2\sigma}$). Albeit at a slower pace, also the radial density increases, given that the radial distance between two consecutive turns would contract as $2\Delta_r \simeq 1/N^\sigma - 1/(N+2m)^\sigma = \frac{1}{N^\sigma} \left(1 - \left(1 + \frac{2m}{N} \right)^{-\sigma} \right)$, which, at large t values, is well approximated by $\Delta_r \simeq \pi \sigma / (t N^\sigma)$. As an example, for $t > 1000$ and along $\sigma = 1/2$, that would correspond to $\Delta_r <$ about 0.3% of r . Hence, at sufficiently large t , the radial density is well approximated by $1/\Delta_r \simeq N^\sigma \frac{t}{\pi \sigma}$ (while it is $N > \frac{t^2}{2\sigma}$).

We shall now remark how the remainder $R'_k(s)$ of the series for the first derivative of the Dirichlet η function, $\eta'(s) = \eta'_{k-1}(s) + R'_k(s)$, also follows a spiraling pattern very similar to that in Fig 4b. Indeed:

Corollary 1. For $s = \sigma + it$ in the interior of the critical strip, denote by $\eta'_{n-1}(s)$ the $(n-1)^{\text{th}}$ partial sum of the series for the first derivative of the η function, and by $R'_n(s)$ the corresponding remainder. The following strict asymptotic relationship holds

$$(16) \quad \text{as } n \rightarrow \infty \quad R'_n(s) = \frac{(-1)^n \log n}{2n^s} + \delta_n(s), \quad \frac{\delta_n(s)}{n^{-\sigma} \log n} \rightarrow 0$$

actually, one even has $\delta_n(s) \in o\left(\frac{\log n}{n^2}\right)$.

PROOF. As $n \rightarrow \infty$, it is $\log(n+1) = \log n + 1/n + \dots$ and $\log(n+2) = \log n + 2/n + \dots$. Retracing then the same geometric proof as for **Theorem 1**, we will obtain, for both the Δ_C and the Δ_r expressions, a first part composed of all terms multiplied by the common factor $\log n$, added to a second part where the same terms are instead multiplied by either $1/n$ or $2/n$, and which will hence vanish at a much faster rate than said first part. \square

Because at sufficiently large values of t and N we have $\log(N+2m)/\log N \sim 1 + \log(1 + \frac{2\pi}{t})/\log N$ (see (15) above), for the first turn of *Deep Spiral N* it will be $\log(N+2m) \simeq \log N$, so we may just as well replace $\log n$ in (16) by $\log N$ (or, for that matter, by $\log(N+2m)$) and still maintain good accuracy. Indeed, if we were to plot the *Deep Spiral N* for the $R'_n(s)/\log N$, at a sufficiently large N we will observe an almost perfect overlap with the *Deep Spiral N* for the $R_n(s)$.

Moreover, if $\eta(s_0) = 0$, and $\Re(s_0) > 0$, observing that the sequence of partial sums $\{\eta_k(z)\}$ converges uniformly on compact subsets of the half-plane $\Re(z) > 0$ to $\eta(z)$, and that for $\eta(z)$ it is possible to find a sufficiently small circular boundary $|z - s_0| = \varepsilon$ surrounding only the s_0 zero (zeros are isolated), while along said boundary it is also $\eta(z) \neq 0$, a known result due to Hurwitz [6] implies that there is an integer N such that for $n \geq N$, $\eta(z)$ and $\eta_n(z)$ have the same number of zeros inside the domain encircled by $|z - s_0| = \varepsilon$ (counting multiplicities is implied). There must hence exist a sequence $\{z_k(s_0)\}$ such that $\eta_{k-1}(z_k(s_0)) = 0$, whereby $z_k(s_0) \rightarrow s_0$ as $k \rightarrow \infty$, s_0 representing an accumulation point for the sequence $\{z_k(s_0)\}$. Denoting by $s_0 = \sigma_0 + it_0$ a zero of the η function, and referring to the even-indexed Hurwitz zeros sub-sequence $\{z_{2k}(s_0)\}$, $z_{2k}(s_0) \rightarrow s_0$ as $k \rightarrow \infty$, defined so that $\eta_{2k-1}(z_{2k}) = 0$, and which in general does not correspond to $\eta_{2k-1}(1 - z_{2k}) = 0$, by definition implies that $\eta(z_{2k}) = R_{2k}(z_{2k})$ (see 4). Now, trying to directly prove that sequences $\{z_{2k}(s_0)\}$, featuring the properties just described, can only exist when $\sigma_0 = 0.5$ appears challenging. However, by combining the results of **Theorem 1** with the constraints imposed by the Functional Equation yields a perhaps easier to approach strict equality.

Corollary 2. *In the interior of the critical strip, the falsehood of the Riemann Hypothesis requires the existence of at least one sequence $\{z_{2k}(s_0)\}$, $\Re(s_0) \neq 1/2$, such that the following equality is eventually satisfied*

$$(17) \quad \eta_{2k-1}(1 - z_{2k}(s_0)) = \chi^\pm(z_{2k}(s_0))R_{2k}(z_{2k}(s_0)) - R_{2k}(1 - z_{2k}(s_0))$$

PROOF.

By the definition of $\{z_{2k}(s_0)\}$, it is $R_{2k}(z_{2k}) = \eta(z_{2k})$. The functional equation $\eta(1 - z_{2k}) = \chi^\pm(z_{2k})\eta(z_{2k})$, considering that $\eta(1 - z_{2k}) = \eta_{2k-1}(1 - z_{2k}) + R_{2k}(1 - z_{2k})$, leads then to (17) in a straightforward way. \square

Conversely, if one can prove that no sequence of Hurwitz zeros $z_{2k}(s_0)$ satisfies the strict equality above, then the Riemann Hypothesis is confirmed. To that aim, a sufficient condition would be to show that the asymptotic behaviours of the two sides of (17) cannot possibly match as $k \rightarrow \infty$.

Denote $z_{2k}(s_0) = s_0 + \delta_{2k}(s_0)$. To rewrite the strict equality above in terms of the asymptotic behaviour of the vanishing left- and right-hand terms, we use the power series expansion of the analytic function on the left-hand side together with the result of **Theorem 1**. This yields the following asymptotic equivalence (the dots denote higher-order terms vanishing at faster rates):

$$(18) \quad \eta_{2k-1}(1 - s_0) - \eta'_{2k-1}(1 - s_0)\delta_{2k} + \dots = -\frac{\chi^\pm(s_0 + \delta_{2k})}{2(2k)^{s_0 + \delta_{2k}}} + \frac{1}{2(2k)^{1 - s_0 - \delta_{2k}}} + \dots$$

At present, however, this seems to be little more than an interesting curiosity, as it remains unclear whether it can meaningfully aid in studying the Riemann Hypothesis. Any progress in this direction would first require a detailed analysis of the asymptotic behaviour of the two partial sums on the left, a daunting task indeed.

3. A REFORMULATION OF THE RIEMANN HYPOTHESIS

Theorem 2. *The statement that $\lim_{n \rightarrow \infty} X_n^\pm(s) = L(s)$ is continuous on $D = \{s \in \mathbb{C} : 0 < \Re(s) < \frac{1}{2}\}$ is a necessary and sufficient condition for the following inequality to be satisfied in D*

$$\eta(s) \neq 0.$$

PROOF. In order to prove necessity and sufficiency, we are going to follow these two logical steps:

- (1) assuming that the Riemann Hypothesis is true, prove that $L(s)$ is continuous,
- (2) assuming that the Riemann Hypothesis is not true, prove that $L(s)$ cannot be continuous.

Starting with the first logical step, the hypothesis $\eta(s) \neq 0$ implies that for sufficiently large n also $\eta_n(s) \neq 0$, so that the limit of the following ratio is eventually properly defined. Moreover, because by definition both $\eta_n(s)$ and $\eta_n(1-s)$ converge point wise to $\eta(s) \neq 0$ and $\eta(1-s) \neq 0$:

$$(19) \quad L(s) = \lim_{n \rightarrow \infty} X_n^\pm(s) = \lim_{n \rightarrow \infty} \frac{\eta_n(1-s)}{\eta_n(s)} = \frac{\lim_{n \rightarrow \infty} \eta_n(1-s)}{\lim_{n \rightarrow \infty} \eta_n(s)} = \frac{\eta(1-s)}{\eta(s)} = X^\pm(s),$$

which is a continuous function on all D .

In order to then prove also the second logical step, let us suppose that there exists $s_0 \in D$ such that $\eta(s_0) = 0$, and consequently also $\eta(1-s_0) = 0$, hence resulting in an undefined ratio. By observing that $\eta(s_0) = 0$ implies $\eta_{n-1}(s_0) = -R_n(s_0)$, and similarly so for $\eta_{n-1}(1-s_0) = -R_n(1-s_0)$, both $\neq 0$, switching to their polar forms, and recalling **Theorem 1**, shows that the limit $L(s_0)$ exists nonetheless ($0 < \sigma_0 < \frac{1}{2}$):

$$(20) \quad L(s_0) = \lim_{n \rightarrow \infty} X_n^\pm(s_0) = \lim_{n \rightarrow \infty} \frac{|\eta_{n-1}(1-s_0)|}{|\eta_{n-1}(s_0)|} e^{i\Delta_n} = \lim_{n \rightarrow \infty} \frac{|R_n(1-s_0)|}{|R_n(s_0)|} e^{i\Delta_n} = \lim_{n \rightarrow \infty} \frac{n^{\sigma_0}}{n^{1-\sigma_0}} e^{i\Delta_n} = 0$$

to then coincide with $X^\pm(s)$ at any other neighboring point $s \neq s_0$ (zeros of analytic functions are isolated). It is known that $X^\pm(s) \neq 0$ throughout the interior of the critical strip, with $X^\pm(s) = 1$ along the critical line, we thus have that $L(s)$ cannot possibly be continuous at $s = s_0$, instead featuring the removable discontinuity $L(s_0) = 0$. \square

Note how **Theorem 2** cannot provide any additional information about zeros located along the critical line. For such zeros, (19) and (20) would both yield $L(s) = 1$, with no discontinuities.

Moreover, **Theorem 2** indicates $L(s_0) = 0$ as the only possible value at discontinuities, if any. Thus, were it possible to prove, from more general properties of the $\eta_n(s)$ sums, that $\lim_{n \rightarrow \infty} X_n^\pm(s) \neq 0$ everywhere inside the left half of the critical strip, and in so doing proving that $L(s)$ must hence be continuous, then the Riemann Hypothesis would be confirmed. We may finally observe that were the non-trivial zeros simple, then the first derivatives $\eta'(s_0)$ and $\eta'(1-s_0)$ would both be $\neq 0$, thus allowing the application of the L'Hôpital's rule in (19) to obtain the nested limit:

$$(21) \quad \lim_{s \rightarrow s_0} \lim_{n \rightarrow \infty} X_n^\pm(s) = \lim_{s \rightarrow s_0} \frac{\eta(1-s)}{\eta(s)} = \frac{\eta'(1-s_0)}{\eta'(s_0)} = X^\pm(s_0),$$

while (20) may also be written as a nested limit:

$$(22) \quad \lim_{n \rightarrow \infty} \lim_{s \rightarrow s_0} X_n^\pm(s) = \lim_{n \rightarrow \infty} \frac{|\eta_n(1-s_0)|}{|\eta_n(s_0)|} e^{i\Delta_n} = 0$$

Thus, were the Riemann Hypothesis wrong, then the two limiting operations (21) and (22) would yield differing results, and they cannot therefore be interchanged. However, were it possible to prove, from more general properties of the $\eta_n(s)$ sums, that the sequence $X_n^\pm(s)$ converges uniformly on D , then said two limiting operations would instead need to be interchangeable, so that assuming the Riemann Hypothesis wrong would lead to a contradiction.

FIGURE 5. The Hurwitz zeros sub-sequence $\{z_{2k}(s_0)\}$ brought to life.

4. FINAL REMARKS

Key implications of the existence of the above introduced Hurwitz zeros sub-sequence $\{z_{2k}(s_0)\}$, whereby $z_{2k}(s_0) = s_0 + \delta_{2k}(s_0)$, $\delta_{2k}(s_0) = \lambda_{2k}(s_0) + i\tau_{2k}(s_0)$, can be effectively visualized by means of the animation in Fig. 5 (it starts automatically in Adobe Acrobat Reader). For the example s_0 = the sixth known zero, and restricting to indexes $N \leq 2k \leq N + 2m$, where $N = 1500$, $2m = 270$ ($2m$ as introduced in (15), and which we may now conveniently refer to as the 2π angular span), the corresponding 135 individual elements of the $\{z_{2k}(s_0)\}$ sequence were at first meticulously assembled using a numerical successive approximations method aiming at $\eta_{2k-1}(z_{2k}) = 0$, or very nearly so. The animation helps illustrate what is going on with said set of 2π angular span indexes:

- The black dots are the $\eta_{2k-1}(s_0) = -R_{2k}(s_0)$, shown for $N \leq 2k \leq N + 2m$ (a 2π angular span).
- The larger gray dot then identifies the particular $\eta_{2k-1}(s_0)$ value which is being moved to the origin when s_0 is switched to $z_{2k} = s_0 + \delta_{2k}$.
- The small gray dots illustrate how all the $\eta_{2j-1}(s_0)$ 135 values consequently also move to their respective new positions $\eta_{2j-1}(s_0 + \delta_{2k})$.
- The animation hence shows how the *Deep Spiral* 1500 first 2π turn moves around when the $z_{2k}(s_0)$ 135 values are sequentially scanned through.

We can observe the following:

- When the gray turn moves around while the $z_{2k}(s_0)$ 135 values are sequentially scanned through, its orientation with respect to the stationary black turn (i.e., the $\eta_{2k-1}(s_0)$) remains practically unaltered, i.e., when the black dot marked by the larger overlapping gray dot is moved to the origin, then also all other dots follow along lines parallel to the line joining the larger gray dot to the origin.
- This is not a feature of the particular zero considered for this example, but it is of very general applicability to all non-trivial zeros. Such a behavior has a simple geometric explanation. Returning for a moment to Fig. 4a, the argument of each one of the black segments (i.e., the various $u_k(s_0)$) is a function of k and t_0 only, i.e., $Arg(u_k(s_0)) = t_0 \log k$. Because s_0 is an accumulation point for the $\{z_{2k}(s_0)\}$, we can always pick a sufficiently large N such that the $\{\tau_{2k}(s_0)\}$ values are guaranteed to be just a tiny fraction of t_0 . When restricting to the interval of k values of interest, the ones covering a full t_0 ($\log(N + 2m) - \log N$) corresponding to a 2π angular span, the above in turn implies that the $\tau_{2k}(s_0)$ ($\log(N + 2m) - \log N$) values can at most correspond to just a tiny fractions

of 2π (vanishing small fractions as $N \rightarrow \infty$). Hence, when switching from t_0 to $t_0 + \tau_{2k}(s_0)$, provided that N is sufficiently large so that over a 2π angular span the τ_{2k} values become just a tiny fraction of t_0 , the relative orientation of said segments (and thus of each of the 135 gray turns revolving the black turn of Fig. 5) can be affected by a tiny amount at most, vanishingly small as $N \rightarrow \infty$.

Observing that by the very definition of $\{z_{2k}(s_0)\}$, it is $R_{2k}(z_{2k}(s_0)) = \eta(z_{2k}(s_0))$, while (10) asymptotically locates the $R_{2k}(z_{2k}(s_0))$ very nearly at the center of the corresponding gray turn, we finally obtain the important result that for sufficiently large N values, over any range $N \leq 2k \leq N + 2m$ which results in the $\eta_{2k}(s_0)$ covering a 2π angular span, $\eta(z_{2k}(s_0))$ will consequentially circle once around the origin. Moreover, since $\eta(s)$ is analytic and the density of the points $z_{2k}(s_0)$ increases with k (both radially and angularly; see the discussion following (15)), we expect that, for s lying on the line segment joining $z_{2k}(s_0)$ and $z_{2k+2}(s_0)$, the value of $\eta(s)$ will lie between the sampled values $\eta(z_{2k}(s_0))$ and $\eta(z_{2k+2}(s_0))$. This last result is key to a deeper geometric understanding of the Simple Zeros Conjecture.

We shall now seek to cast the preceding argument in a more formal framework.

Because s_0 is an accumulation point for $\{z_{2k}(s_0)\}$, let us write $z_{2k}(s_0) = \sigma_0 + \lambda_{2k}(s_0) + i(t_0 + \tau_{2k}(s_0)) = s_0 + \delta_{2k}(s_0)$, $\lambda_{2k}(s_0) \rightarrow 0$ and $\tau_{2k}(s_0) \rightarrow 0$ as $k \rightarrow \infty$. Thus, simplifying notation by omitting the dependence on s_0 when not needed, and recalling that each $R_n(s)$ is analytic, so that $R_{2k}(z_{2k}) = R_{2k}(s_0) + R'_{2k}(s_0)\delta_{2k}(s_0) + \dots$ (reminding that the z_{2k} are the values at which $\eta(z_{2k}) = R_{2k}(z_{2k})$), (10) and (16) yield ($\sigma_0 + \lambda_{2k} > 0$)

$$(23) \quad \eta(z_{2k}) = \frac{-1}{2(2k)^{z_{2k}}} + o\left(\frac{1}{k^2}\right) = \frac{-1}{2(2k)^{s_0}} + \frac{\log(2k)}{2(2k)^{s_0}} \delta_{2k}(s_0) + \dots + o\left(\frac{\log k}{k^2}\right)$$

As $\tau_{2k} \rightarrow 0$ ($k \rightarrow \infty$), the argument of the term on the left-hand side, $(t_0 + \tau_{2k})\log(2k)$, approaches and increasingly overlaps with the argument of the first term on the right-hand side, $t_0 \log(2k)$. This does not happen for the second term because of the argument of $\lambda_{2k} + i\tau_{2k}$, i.e., $\arctan(\tau_{2k}/\lambda_{2k})$, which can cause the two terms to be nearly in phase for some values of k and in opposition for others, while also allowing intermediate phase values. Eventually, both sides of this asymptotic equivalence must vanish at the same rate. This requires that λ_{2k} and τ_{2k} vanish faster than $1/\log(2k)$, that is, $\lambda_{2k} \in o(1/\log(2k))$, which hence imposes a lower bound on the rate at which the values $\{z_{2k}(s_0)\}$ converge to s_0 . Therefore, as we move along the sequence $\{z_{2k}(s_0)\}$, the corresponding $\eta(z_{2k}(s_0))$ values can be approximated - with increasing accuracy as k increases - by the first term on the right-hand side of (23). Although k^{-s} , for fixed k , is an analytic function of s , this is not the case for $k^{-z_{2k}}$, since in this expression the base k varies together with the exponent. Hence, equation (23) does not represent the analytic function $\eta(s)$ itself. Rather, it should be understood as providing the simple expression $-(2k)^{-s_0}/2$ as an approximation for discrete values of $\eta(s)$ sampled at the points $s = z_{2k}(s_0)$, with the accuracy of the approximation improving as k increases.

Now denote by γ_N (N , j , and m defined as in (15)) the polygon whose vertices are

$$(24) \quad v_N = s_0 + \frac{-e^{-it_0 \log N}}{c 2N^{\sigma_0}}, \dots, v_{N+2j} = s_0 + \frac{-e^{-it_0 \log(N+2j)}}{c 2(N+2j)^{\sigma_0}}, \dots, v_{N+2m} = s_0 + \frac{-e^{-it_0 \log(N+2m)}}{c 2(N+2m)^{\sigma_0}}$$

$c \in \mathbb{C}$, $c \neq 0$, as yet undetermined, and where the last side of the polygon is drawn between the v_m and v_0 vertices, thus resulting in a piecewise linear, simple closed curve. The γ_N polygon features the following properties:

- The discussion following (15) implies that, at sufficiently large N , the length of the sides of γ_N , $|v_{N+2j+2} - v_{N+2j}| \simeq t_0/(N+2j)^{1+\sigma_0}$, is much smaller than $|v_{N+2j} - s_0| \simeq \frac{1}{2}/(N+2j)^{\sigma_0}$. Thus, the angular density of vertices is a monotonically increasing function of N . A different approximation instead applies to their radial density, which is governed by $|v_N - v_{N+2m}| \simeq \pi\sigma_0/(t_0 N^{\sigma_0})$. This quantity is also much smaller than $|v_{N+2j} - s_0|$, although now only by the fixed ratio $2\sigma_0\pi/t_0$ (an approximation valid for sufficiently large t_0 values).
- Since the zeros of analytic functions are isolated, there always exists an N sufficiently large such that s_0 is the only zero encircled by γ_N (while also recalling that, in the interior of the critical strip, there exists a region $0 \leq \sigma < f(t)$ that is known to be free of zeros).

All γ_N are therefore simple, piecewise linear, polygonal closed curves. By sampling the analytic function $c(s - s_0)$ at the vertices of γ_N , and using equation (23), we obtain the following discrete set of values:

$$(25) \quad c(v_{N+2j} - s_0) = \frac{-e^{-it_0 \log(N+2j)}}{2(N+2j)^{\sigma_0}} = \eta(z_{2N+2j}) + \text{err}(v_{N+2j}), \quad \lim_{N \rightarrow \infty} \frac{|\text{err}(v_{N+2j})|}{|v_{N+2j} - s_0|} = 0, \quad 0 \leq j \leq m$$

Asymptotically, the main contribution to $\text{err}(v_{N+2j})$ comes from the second term on the right-hand side of (23). Observing that $|v_{N+2j} - s_0| = (N+2j)^{-\sigma_0}/2$, we then verify the limit at the right. It thus follows that, when a full turn is completed around γ_N , the discrete value $\eta(z_{2N+2j})$ completes one full turn around 0. Because $\eta(s)$ is an analytic function, and since the density of the vertices of γ_N increases with N , we may therefore expect that along the sides of γ_N the function $\eta(s)$ takes values interpolated between $\eta(z_{2N+2j})$ and $\eta(z_{2N+2j+2})$. It is therefore reasonable to expect that the winding number of $\eta(s)$ around 0 coincides with that of γ_N around s_0 , which is equal to 1 or -1 , depending on the orientation, since γ_N is a simple closed curve. In a more formal approach, we expand $\eta(s)$ in a power series around s_0 , evaluating it along γ_N :

$$(26) \quad \eta(s_{\gamma_N}) = \eta'(s_0)(s_{\gamma_N} - s_0) + \eta''(s_0)(s_{\gamma_N} - s_0)^2/2 + \dots$$

To ensure that the asymptotic equivalence (25), which holds at the vertices of γ_N (24) and was derived from (10) and (16) in a manner completely independent of the validity of (26), is satisfied, it is necessary that $\eta'(s_0) = c$. Consequently, we must have $\eta'(s_0) \neq 0$, i.e., the zero s_0 is simple. It then follows that along the entire curve γ_N we have

$$(27) \quad \eta(s_{\gamma_N}) = \eta'(s_0)(s_{\gamma_N} - s_0) + \text{error}(s_{\gamma_N}), \quad \lim_{N \rightarrow \infty} \frac{|\text{error}(s_{\gamma_N})|}{|s_{\gamma_N} - s_0|} = 0$$

where $\text{error}(s_{\gamma_N})$ collects the various error terms, including those arising from (23) and those corresponding to higher-order terms in the power series expansion of $\eta(s)$. Moreover, by replacing $c = \eta'(s_0)$ in (24), we obtain a sequence of values which approximate the values of the Hurwitz zeros sequence $\{z_{2k}(s_0)\}$ with increasing accuracy as $k \rightarrow \infty$. To obtain a direct sense of the approximation's accuracy through straightforward numerical computations, one may simply substitute the values of the sequence (24) into the partial sums $\eta_{2k-1}(z_{2k})$ and then examine how close to zero they are, for example relative to a meaningful reference scale such as $1/(2k)^{\sigma_0}$.

REFERENCES

- [1] Riemann, Bernhard. Über die Anzahl der Primzahlen unter einer gegebenen Grösse. PDF copy of the original
- [2] Edwards, H. M. . Riemann's Zeta Function and the Greatest Unsolved Problem in Mathematics, Dover Publications, Mineola, New York (2001)
- [3] Wolf, Marek. Will a physicist prove the Riemann hypothesis? Rep. Prog. Phys. 83 (2020) 036001
- [4] Weisstein, Eric W. "Dirichlet Eta Function." mathworld.wolfram.com/DirichletEtaFunction.html
- [5] Derbyshire, John. Prime Obsession: Bernhard Riemann and the Greatest Unsolved Problem in Mathematics, page 147. Penguin Group, New York (2004)
- [6] John B. Conway. Functions of One Complex Variable, pg. 152 Springer-Verlag, New York, New York, 1978.
- [7] Krantz, S. G.. Handbook of Complex Variables, p. 74. Birkhäuser, 1999. Boston